VLA Test Memo. No. 222

Phase Fluctuations at the VLA Derived From One Year of Site Testing Interferometer Data

Bryan Butler & Ketan Desai
National Radio Astronomy Observatory

October 1, 1999

Introduction

In order to test fluctuations in phase at the VLA site, a site testing interferometer (STI) was installed there around the beginning of 1998. The STI measures phase by observing a geostationary satellite beacon (at 50° elevation) at 11.3 GHz with two 1.8 m satellite dishes separated by 300 m. Radford *et al.* (1996) give a general description of the instrument, and Carilli *et al.* (1998) describe some of the specifics of the VLA STI. Since the STI has been operating for more than a year at the VLA site, it seems an appropriate time to investigate the statistics of phase fluctuations measured by it over that time span.

Overview

The analysis of data from an STI is described in several places, including Carilli *et al.* (1998), Holdaway *et al.* (1997), Radford *et al.* (1996), Holdaway *et al.* (1995), and Ishiguro *et al.* (1989). We will not describe in detail the particular quantities we derive and discuss in this memo, but refer the reader to these references and give only a brief description here.

Given a time series of phases from the STI, some interesting derivable quantities are: the rms phase (ϕ_{rms}^{STI}); the power law exponent of the temporal phase structure function at small lags (β); and the corner time (t_{corner}). In this memo we work with the structure function, rather than the root structure function discussed by Holdaway *et al.* (1995), and we note that the rms phase is related to the "saturation phase" (ϕ_{sat}) as: $\phi_{sat} = \sqrt{2}\,\phi_{rms}^{STI}$ (as also noted in Carilli *et al.* [1998]), and that the power law exponent we use is related to that of Holdaway *et al.* (1995) as: $\beta = 2\alpha$. We derive these quantities with a method somewhat different than that described in Holdaway *et al.* (1995), and so get slightly different answers. Because the method is different, it deserves explanation.

Given the time series of phase, we derive the three quantities of interest in the following steps:

- unwrap the phases
- fit and remove the satellite drift as a 2^{nd} order polynomial in the phase time series
- calculate the rms of the phase time series (ϕ_{rms}^{STI})
- form the log structure function (log temporal phase structure function vs log lag)
- fit for β as the slope of the log structure function using only those lags for which the structure function value is less than $(\phi_{rms}^{STI})^2$, and calculate $\alpha = \beta/2$
- calculate t_{corner} as the time when the above fit equals $2\,(\phi_{rms}^{STI})^2$

In general, we find that the power law slopes derived in this way are somewhat higher than with the method of Holdaway *et al.* (1995), and hence the corner times are smaller. Figure 1 shows an example of a phase structure function, with our new fit values drawn as a solid line and the fit values derived using the scheme of Holdaway *et al.* as a dashed line. We have investigated trying to fit for and remove an electronic noise term (as discussed in Holdaway *et al.*), but found it unneccessary (the electronic noise term is very small compared to the first lag in the structure function even under the best atmospheric conditions and so it is not possible to fit reliably for it).

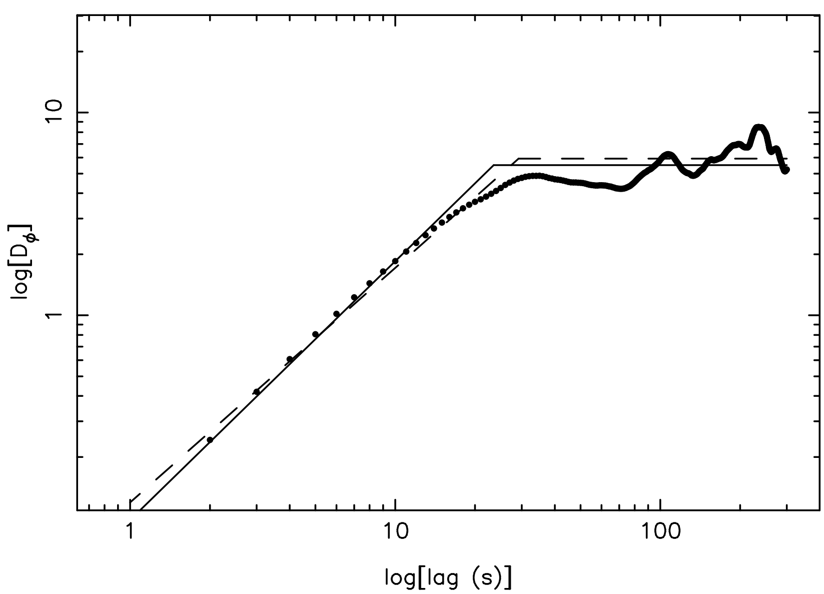

Figure 1: Log structure function, using 10 minutes of data from 07Jan1999. Also shown are fits using our method (solid line) and the Holdaway *et al.* (1995) method (dashed line).

Data

We present here analysis of data taken from 01Sep1998 to 31Aug1999 inclusively. Note that there are some significant gaps in the archival data (notably Feb1999 has little data), but we feel that this is a representative dataset. For each day when the STI is functioning correctly, there are 2 raw data files which contain the STI data. These files are converted into a format which can be read into a FORTRAN program which calculates the values of ϕ_{rms}^{STI}, t_{corner}, and α. Given a string of phases for long stretches (half a day nominally), the program takes the first 10 minutes of data and calculates the 3 values according to the algorithm above. It then advances by 5 minutes and does the same, repeating this until the end of the file is reached. The day, time of day, and 3 values are then written into a file for further processing. This involves taking the values and binning them according to month and daytime or nighttime. Daytime and nighttime values are distinguished by calculating the time of sunrise and set for each day and checking whether the sun is up or not. Fits are rejected if the original STI data indicates that the amplitudes were low, or if the fit rms phase is $> 50°$.

We present values for the cumulative distributions for each month, separated into daytime and nighttime, at the 10^{th}, 50^{th}, and 90^{th} percentiles, shown in Table 1.

Discussion

Similar to Dick Sramek's earlier findings, we find that the phase fluctuations at the VLA site group themselves naturally into several seasonal and diurnal groups (Sramek 1983, 1989). Dick had broken the phase stability into 3 general regimes: winter nighttime; winter daytime and summer nighttime; and summer daytime. We find the same general trend, but prefer to split it into 4 general groups in the following seasons: winter – Dec to Feb; spring – Mar to Jun; fall – Oct and Nov; and summer – Jul to Sep. The groupings of phase stability then fall into these 4 categories:

- winter nighttime — $2° \lesssim \text{ median } \phi_{rms}^{STI} \lesssim 2.5°$
- winter daytime and spring and fall nighttime — $2.5° \lesssim \text{ median } \phi_{rms}^{STI} \lesssim 4.5°$
- summer nighttime and spring and fall daytime — $4.5° \lesssim \text{ median } \phi_{rms}^{STI} \lesssim 8°$
- summer daytime — median $\phi_{rms}^{STI} \gtrsim 10°$

Recall that these phase fluctuations are near 50° elevation, on a 300 m baseline, and at 11.3 GHz frequency, so expectations for observations at other elevations, baseline lengths, and frequencies should be scaled accordingly. Following Carilli *et al.* (1998) and adding the expected dependence on elevation, we write for the rms phase after calibration on a VLA observation:

$$\phi_{rms}^{VLA} = \frac{1.9}{\lambda_{cm}} \left(\frac{t_{cycle}}{2\,t_{corner}}\right)^{\alpha} \sqrt{\frac{A_{VLA}}{A_{STI}}}\,\sqrt{2}\,\phi_{rms}^{STI} \quad ,$$

Table 1: Summary of values derived from STI data taken from 01Sep1998 to 31Aug1999.

				ϕ_{rms}^{STI}			t_{corner}			α	
month	day/night	n_{samp}	10%	50%	90%	10%	50%	90%	10%	50%	90%
1	d	3519	1.5	3.8	8.9	13.1	21.7	42.9	0.56	0.66	0.74
1	n	4852	1.3	2.5	6.4	11.9	20.1	39.6	0.54	0.63	0.72
2	d	667	1.7	3.7	7.9	14.1	22.5	43.0	0.57	0.65	0.72
2	n	956	1.1	2.1	5.6	12.4	22.8	42.4	0.53	0.61	0.70
3	d	3070	1.9	5.2	13.2	16.5	27.5	47.6	0.56	0.66	0.74
3	n	3246	1.3	2.7	5.7	13.9	23.4	47.3	0.51	0.62	0.70
4	d	3695	2.5	6.7	13.9	14.1	22.0	39.8	0.57	0.66	0.74
4	n	3191	1.4	3.1	7.0	12.1	19.8	36.5	0.53	0.63	0.71
5	d	2945	2.3	6.3	15.9	14.0	24.7	43.9	0.57	0.67	0.74
5	n	2383	1.4	3.0	9.7	11.9	20.3	37.8	0.54	0.63	0.73
6	d	3298	2.6	7.6	19.4	18.3	30.3	51.1	0.59	0.68	0.76
6	n	2288	1.5	3.4	6.9	17.6	28.1	49.1	0.55	0.64	0.72
7	d	2210	3.6	10.0	25.1	25.2	39.3	62.2	0.61	0.70	0.78
7	n	1543	3.0	5.5	12.3	22.1	35.4	58.9	0.58	0.67	0.74
8	d	4705	4.2	11.9	27.8	22.6	36.8	59.0	0.60	0.70	0.77
8	n	3802	3.3	6.2	14.1	22.2	35.1	57.0	0.59	0.68	0.75
9	d	2890	5.6	13.6	28.4	19.7	31.7	52.0	0.61	0.70	0.78
9	n	2983	3.3	6.1	13.3	16.7	27.6	47.9	0.58	0.68	0.75
10	d	1724	2.8	8.1	16.1	15.6	25.3	47.0	0.57	0.66	0.74
10	n	2090	1.6	4.3	9.9	14.8	24.1	44.0	0.56	0.65	0.73
11	d	1481	2.0	5.5	16.1	16.3	27.5	49.8	0.57	0.67	0.75
11	n	1860	1.8	3.8	8.8	12.4	20.8	39.5	0.56	0.64	0.73
12	d	1995	1.3	3.4	6.9	14.6	27.1	52.9	0.54	0.63	0.73
12	n	2737	1.0	2.2	5.0	13.7	24.4	51.7	0.51	0.62	0.71

where t_{cycle} is the calibration cycle time, A_{STI} is the airmass of the STI satellite ($A_{STI} \sim 1/\sin E_{STI} \sim 1.3$), and A_{VLA} is the airmass of the observation. So, most of the STI measured values can be combined into the quantity:

$$\sqrt{C_n^2} = \frac{\sqrt{2}\,\phi_{rms}^{STI}}{t_{corner}^{\alpha}} \quad ,$$

which is a relative measure of phase stability at the VLA. Table 2 shows the values for the cumulative distribution for this value for each month, separated into daytime and nighttime, at the 10^{th}, 50^{th}, and 90^{th} percentiles. Note that the same 4 general groupings hold as above with median $\sqrt{C_n^2}$ ranges of: 0.4-0.55; 0.55-0.8; 0.8-1.1; and 1.1-1.7, with a few exceptions. Substituting $\sqrt{C_n^2}$, the

Table 2: The quantity $\sqrt{C_n^2}$.

month	daytime 10%	daytime 50%	daytime 90%	nighttime 10%	nighttime 50%	nighttime 90%
1	0.30	0.69	1.60	0.27	0.51	1.39
2	0.33	0.68	1.44	0.23	0.41	1.48
3	0.37	0.82	1.98	0.25	0.57	1.12
4	0.45	1.23	2.60	0.30	0.66	1.51
5	0.41	1.03	2.59	0.31	0.59	2.05
6	0.41	1.06	2.35	0.30	0.55	1.10
7	0.44	1.13	2.43	0.40	0.75	1.56
8	0.55	1.39	3.07	0.45	0.81	1.65
9	0.71	1.68	3.78	0.49	0.95	1.98
10	0.41	1.40	2.81	0.25	0.83	1.88
11	0.35	0.88	2.15	0.35	0.81	1.65
12	0.24	0.61	1.24	0.20	0.42	1.05

Table 3: rms phase for the VLA at 7 mm after calibration under median conditions.

	ϕ_{rms}^{VLA} (deg)					
	t_{cycle} = 2 mins		t_{cycle} = 5 mins		t_{cycle} = 10 mins	
month	day	night	day	night	day	night
1	25.5	18.8	47.1	34.6	74.7	54.9
2	25.0	15.1	46.1	27.8	73.2	44.2
3	30.2	20.9	55.7	38.4	88.4	61.0
4	45.4	24.5	83.5	45.1	132.6	71.6
5	38.1	21.9	70.1	40.3	111.3	64.0
6	39.1	20.3	72.0	37.5	114.3	59.5
7	41.7	27.6	76.8	50.9	122.0	80.8
8	51.1	29.7	94.1	54.7	149.4	86.9
9	62.0	34.9	114.3	64.3	181.4	102.1
10	51.6	30.8	95.1	56.7	150.9	89.9
11	32.3	29.7	59.5	54.7	94.5	86.9
12	22.4	15.6	41.3	28.8	65.5	45.7

VLA phase is then:

$$\phi_{rms}^{VLA} = \sqrt{C_n^2}\,\frac{1.9}{\lambda_{cm}}\,\sqrt{\frac{A_{VLA}}{A_{STI}}}\,\left(\frac{t_{cycle}}{2}\right)^{\alpha} \quad .$$

To simplify this relationship further, assume that $\sqrt{A_{VLA}/A_{STI}} \sim 1$, and that $\alpha \sim 2/3$ (true for median conditions at least), then we have:

$$\phi_{rms}^{VLA} = \frac{\sqrt{C_n^2}\,t_{cycle}^{2/3}}{\lambda_{cm}} \quad ,$$

which can be used as a rough rule of thumb for planning purposes. Table 3 shows values of this quantity for an observation at a wavelength of 7 mm for 3 different cycle times: 2, 5, and 10 minutes. The median values from Table 2 were used in the calculation.

Acknowledgements

Simon Radford and Gerry Petencin designed and built much of the STI. Scott Foster and Mark Holdaway provided early software and ideas on data analysis. Tom Folkers, Phil Dooley, Alan Roy, and Chris Carilli made specific contributions to the VLA STI.

References

Carilli, C.L., M.A. Holdaway, & A. Roy, Calibrating the Site Testing Interferometer, VLA Test Memo. No. 213, 1998

Holdaway, M.A., S. Matsushita, & M. Saito, Preliminary Phase Stability Comparison of the Chajnantor and Pampa la Bola sites, MMA Memo. No. 176, 1997

Holdaway, M.A., S.J.E. Radford, F.N. Owen, & S.M. Foster, Data Processing for Site Test Interferometers, MMA Memo. No. 129, 1995

Ishiguro, M., T. Kanzawa, & T. Kasuga, Monitoring of Atmospheric Phase Fluctuations Using Geostationary Satellite Signals, in *Radio Astronomical Seeing*, ed. J.E. Baldwin & W. Shouguan, 1989

Radford, S.J.E., G. Reiland, & B. Shillue, Site Test Interferometer, *PASP, 108*, 441–445, 1996

Sramek, R.A., Atmospheric phase stability at the VLA, VLA Test Memo. No. 175, 1989

Sramek, R.A., VLA Phase Stability at 22 GHz on Baselines of 100m to 3km, VLA Test Memo. No. 143, 1983